Dynamics, Spin Fluctuations, and Bonding in Liquid Silicon

I. Štich,[1] M. Parrinello,[2] and J. M. Holender[3]
[1]*JRCAT, Angstrom Technology Partnership, 1-1-4 Higashi, Tsukuba, Ibaraki 305, Japan*
[2]*Max-Planck-Institut für Festkörperforschung, Heisenbergstrasse 1, 70569 Stuttgart, Germany*
[3]*Department of Physics, Keele University, Keele, Staffordshire ST5 5BG, United Kingdom*
(Received 2 October 1995)

We present a large-scale molecular dynamics simulation of liquid silicon close to the melting point. We find that inclusion of spin has appreciable effects on the description of the bond breaking and forming processes. This improves the description of the structure, significantly modifies the dynamics, and suggests a possible explanation of measured anomalies in properties just above the melting point.

PACS numbers: 61.20.Ja, 61.25.–f, 71.22.+i

Tetravalently bonded semiconductors Si, Ge, and GaAs when melted form rather unusual metallic liquids. As opposed to simple liquids they have a low coordination number (6–7) [1–3] which results from persistence in the melt of covalent bonding. Their diffusivity, when measured, is very high in spite of their covalent character. The semiconductor to metal transition at the melting point is accompanied by a large increase ($\sim$10%) in density [4]. In addition, Si in a range of $\sim$20 K above the melting point exhibits further anomalies in the temperature dependence of density, viscosity, and surface tension [5].

These unusual properties, as well as the relevance of these melts to the crystal growth processes, have attracted a lot of theoretical attention. However, the delicate balance between metallic and covalent behavior has proven rather difficult to model with empirical potentials [6]. For this reason more sophisticated approaches which explicitly take into account the electronic properties have been applied. These were the semiempirical tight-binding (TB) molecular dynamics (MD) approach [7–9] and the fully *ab initio* MD [10–12]. The empirical potentials yielded liquids microscopically different from those generated *ab initio* [10]. The TB approach gave substantially better results but, as we shall show, it is not devoid of problems. Liquid Si (ℓ-Si) has been one of the first systems to which *ab initio* MD has been applied [10]. Those first results were confirmed by a series of other *ab initio* simulations [11,12] which have employed different methodological variants. However, the basic limitations of the first study were not overcome. These were as follows: (1) the neglect of spin effects, (2) the use of a small simulation cell (64 atoms), and (3) the use of the local density approximation (LDA). Especially relevant is the neglect of spin effects. In fact, in ℓ-Si the dominant process is a continuous breaking and forming of covalent bonds in response to the atomic motion [10]. LDA has well-known difficulties in describing bond breaking in molecules [13]. Such a difficulty is clearly reflected in the early simulations, which failed to describe accurately the first coordination shell, that is, the region where chemical bonding takes place.

The purpose of this Letter is as follows: (1) to provide an accurate and reliable description of the structure, bonding, and properties of ℓ-Si which goes well beyond the approximations hitherto attempted; (2) to check the accuracy of the *ab initio* results at several levels of approximation such as LDA [14], generalized gradient approximation (GGA), and spin-polarized GGA (SGGA) [15] which is believed to give a better description of bond breaking and forming processes; and (3) to provide a set of *ab initio* generated coordinates for systems having sizes approaching those customarily used in classical simulations ($\sim$350 atoms) which can be used to interpret and refine the experimental results [16]. We indeed find that inclusion of the spin significantly modifies the attractive part of the interatomic potential and hence has an appreciable effect on the bonding and properties of the liquid. Use of larger simulation cell and GGA has only a small effect.

The simulations have been performed using massively parallel computation [17]. We have chosen to simulate the thermodynamic state $\sim$20 K above the melting point characterized by $T = 1700$ K, $\rho = 2.59$ g/cm^3 [5]. Plane-wave pseudopotential techniques [18] in three different approximations have been used: LDA, GGA, and SGGA. Implementation of the gradient corrected functionals followed Ref. [19]. The Brillouin zone of the MD cell containing 343 atoms was sampled at the Γ point. The wave functions were expanded in plane waves with a cutoff of 10 Ry. The density functionals were minimized to an accuracy of 1×10^{-5} eV/atom. The equations of motion for the ionic degrees of freedom were discretized with a time step of $\sim$3 fsec. We have introduced a Nosé thermostat [20] with dynamical mass of 1.3×10^6 a.u. on the ionic degrees of freedom. The simulations consisted of two longer runs ($\sim$0.9 psec) using LDA and SGGA which were preceded by an equilibration of 0.1 psec. We also made, for checking purposes, a much shorter GGA run ($\sim$0.15 psec). The picosecond MD observation time is justified because typical ionic relaxation times are of the order of 0.1 psec [10]. In preliminary runs we have performed two sets of calculations: one in which the S_z was 0 and one in which S_z was allowed to fluctuate. Both runs gave essentially the same result. Hence we believe that a possible presence of multiple local minima associated with different spin states is statistically irrelevant.

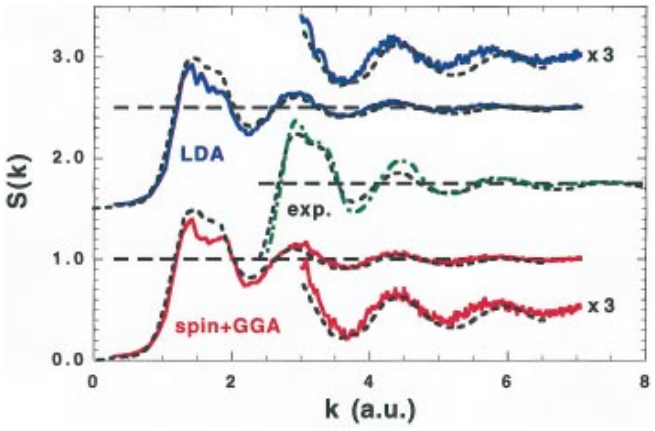

FIG. 1 (color). Static structure factor $S(k)$ in LDA and SGGA compared with experiment [3] (black dashed curve). The insets from the top to the bottom show the comparison between the LDA and experiment [3] for large k on expanded scale, comparison of the two x-ray scattering experiments (black Ref. [3], green Ref. [1]), and comparison between the SGGA and experiment [3] for large k on expanded scale, respectively. Notice that the LDA curve is out of phase with respect to the experiment in the large-k domain.

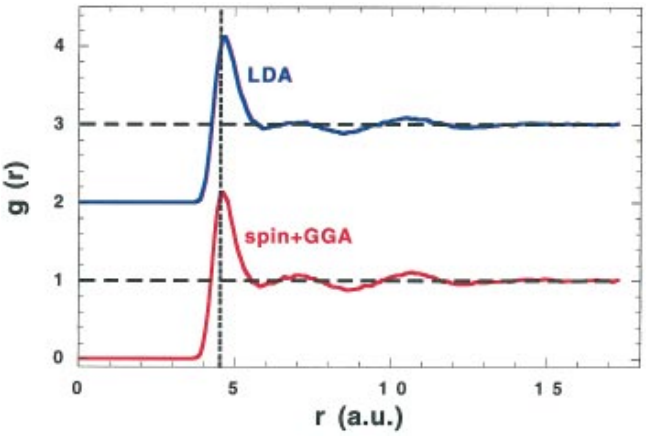

FIG. 2 (color). Pair-correlation function $g(r)$ in LDA and SGGA. The vertical line gives the experimental position of the first peak of $g(r)$.

In Fig. 1 we show the calculated and experimental static structure factors $S(k)$. In both approximations (LDA, SGGA) the calculated results are in good agreement with the new set of x-ray scattering data [3]. Comparison of the two x-ray scattering data [1,3] reveals differences in the heights of the first two peaks and in the low-k edge of the first peak and gives an estimate of the experimental uncertainties. All in all our simulation is more in agreement with the most recent set of experimental data. However, also LDA and SGGA results exhibit differences. The form of the first peak and the shoulder on the high-k side of the first peak are different in the LDA and SGGA. The LDA curve is also slightly out of phase at larger k. Small as they might look, these differences reflect appreciable modification of system bonding and dynamics. Both descriptions yield an asymmetric first peak of $S(k)$ which is a prominent feature of the liquid but the shoulder on the first peak is much more pronounced in the SGGA description. This feature becomes the dominant peak in $S(k)$ of the amorphous Si (a-Si) [21], which suggests that it corresponds to the presence of tetrahedral order in the system. Dephasing of the LDA curve at large k translates into a shift of the first peak of the pair-correlation function $g(r)$ to larger r. Both differences make the LDA liquid less covalent than its SGGA counterpart. We have checked whether these differences stem from the spin or from the gradient corrections. A simulation with the GGA functional (not shown) yielded structural properties virtually identical to those of LDA; hence we conclude that the observed differences are primarily due to the spin.

In real space comparison between theory and experiment is also very favorable. However, in Fig. 2 we focus only on the differences between the $g(r)$ in LDA and SGGA showing only the experimental first peak position of $g(r)$ ($R^{\mathrm{I}}_{\mathrm{exp}} = 4.54$ a.u.) [1,2,22]. In LDA the first peak is shifted to larger r ($R^{\mathrm{I}}_{\mathrm{LDA}} = 4.7$ a.u.) while SGGA brings it closer to experiments ($R^{\mathrm{I}}_{\mathrm{SGGA}} = 4.6$ a.u.). There are also difference in other details. If we define the coordination number by integrating the $g(r)$ up to the first minimum, we obtain 6.7 in LDA as opposed to the SGGA value of 6.2 and the value 6.4 from experiments [1,2,22].

Useful structural information is contained in higher-order correlation functions g_n. It is typically at this level that models based on empirical force models show their limits [6,10]. The calculated g_3 is similar to the one obtained in the earlier *ab initio* simulation [10] with peaks around 60° and 90°. We also measured the dihedral-angle distribution. This is a four-body correlation function which could not be reliably determined in previous *ab initio* simulations because of the small simulation cell then used. The resulting distribution shows small dihedral angles are suppressed and there are very broad maxima at ~60°, 90°, and 180°, very much like the dihedral-angle distribution in rapidly quenched models of a-Si [23].

We now turn to the analysis of the valence electronic charge and spin densities. A qualitative insight may be obtained from Fig. 3. The total charge density is strongly inhomogeneous with covalent bonds between pairs of strongly bonded atoms. Moreover, covalently bonded triplets of atoms show a pronounced tendency towards creation of tetrahedral order. Spin fluctuations localize on weak or dangling bonds and their appearance is precursor to bond breaking or forming. The average total spin is zero but there are large temporal fluctuations in the spin. These in turn correlate with fluctuations in the position and shape of the first peak of the instantaneous $g(r)$. This explains the origin of the differences in the structure of the liquid in the description with and without the spin.

In order to make these observations more quantitative we explore different correlation functions that involve charge and spin density. We will follow a technique described in Ref. [10]; namely, we locate the positions of the local maxima of the charge and spin density with

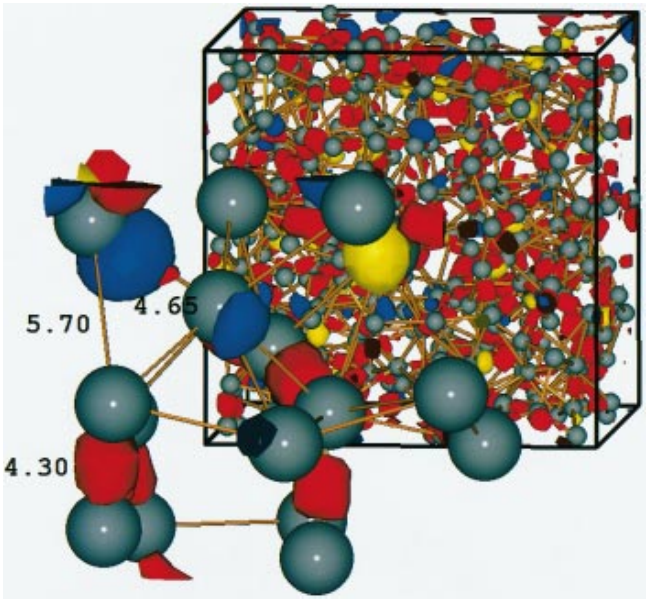

FIG. 3 (color). Snapshot of a low-spin configuration. Superimposed on the ball-stick model are isosurfaces corresponding to the total charge of covalent bonds (red), spin↑ (yellow), and spin↓ density (blue). Superimposed zoom shows the lower left part of the unit cell. Numbers correspond to the lengths (in a.u.) of the bonds. Note the spin fluctuation accompanying formation of a bond in the upper left part of the zoom.

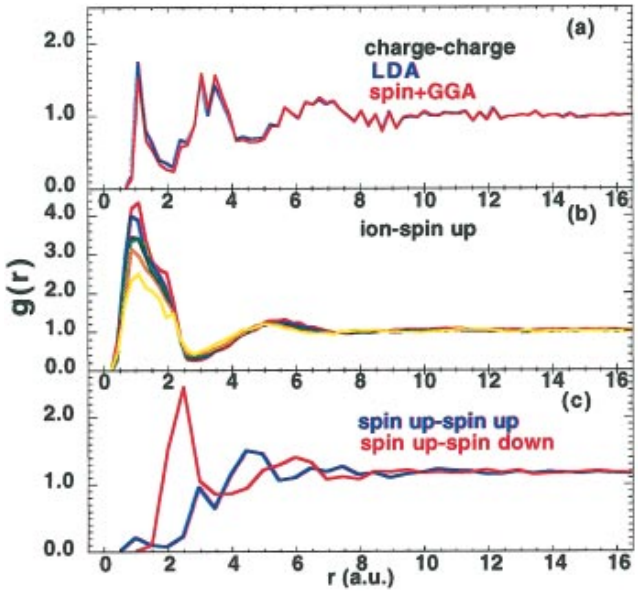

FIG. 4 (color). Characterization of bonding by pair-correlation functions: (a) charge-charge; (b) ion-spin; red, blue, green, orange, and yellow curves correspond to atoms having 0, 1, 2, 3, and 4 covalent bonds, respectively; (c) like-spin (blue); spin up−spin down (red) correlation.

Monte Carlo random walks on the three-dimensional mesh on which these quantities are represented. We then treat these extrema as additional particles and calculate the distribution functions weighting each contribution by the local maximum value. The results for charge-charge, ion-spin↑, spin↑-spin↑, and spin↑-spin↓ density correlations are plotted in Fig. 4. The first prominent peak of the charge-charge correlation at ~1 a.u. corresponds to broken bonds which are characterized by double maxima. This feature is more pronounced in LDA with the weight shifted to larger r, which indicates that the LDA interatomic potential is longer ranged and makes the lifetime of the stretched or broken bonds longer in LDA. The ion-spin correlation peaked at ~1 a.u. shows the dangling-bond character of the spin fluctuations; the like-spin correlation has a weak maximum ~4 a.u. indicating a slight tendency to like-spin clustering. The strong peak in the spin↑-spin↓ correlation at ~2.5 a.u. corresponds to spin↑, ↓ localized on two different bonds of the same atom. In Fig. 5 we give the distribution of the values of the local charge and spin density maxima. Most of the maxima correspond to bonds significantly weaker than in the crystal. An important feature is the shift of the total SGGA charge density distribution to larger values compared to LDA. This again indicates that the bond is more easily broken in the SGGA, thus on average reducing the lifetime of the broken bonds characterized by weaker charge-density maxima.

We have studied the single-particle motion and measured the diffusion coefficient D. To the best of our knowledge the experimental value of D is not yet known. Thus in Table I we can compare only with the results of other calculations. The theoretical estimates vary by a factor of ~4.5 and the value of D increases with the accuracy of the calculation. The SGGA calculation [Fig. 6(a)] gives the highest value of D because introduction of spin facilitates breaking of the bonds, thus lowering the barrier to diffusion. The fact that the barriers are slightly higher in LDA is also reflected in the position of the first peak of $g(r)$. In LDA some of the particles which would have had enough kinetic energy to climb the SGGA barrier are instead bounced back by the higher LDA barriers adding weight to the $g(r)$ in the high-r side of the peak. The velocity-velocity autocorrelation function $Z(t) \propto \langle \vec{v}(0) \cdot$

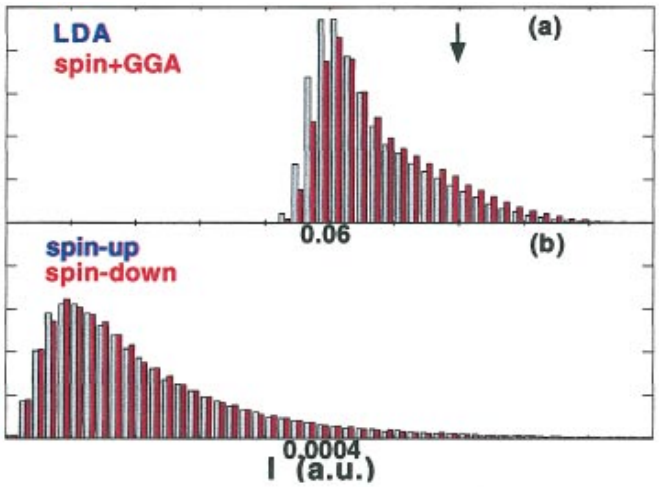

FIG. 5 (color). Distribution of charge and spin density maxima: (a) total charge; (b) spin↑ (spin↓). The arrow indicates the value of the charge density maxima in the crystal.

TABLE I. Computed self-diffusion coefficient D, in 10^{-4} cm^2/s, in the SW, TB, *ab initio* LDA, and SGGA models: (a) Ref. [6], (b) Ref. [7], (c) Ref. [8], (d) Ref. [9], (e) Ref. [11], (f) Ref. [10], and (g) present work.

	SW	TB	LDA	SGGA
D	0.7[a]	1.1[b]	1.9[e]	3.1[g]
		1.3[c]	2.3[f]	
		1.7[d]	2.4[g]	

$\vec{v}(t)\rangle$ in Fig. 6(b) exhibits an unusual feature; namely, it does not cross the positive axis as it would in simple dense liquid as a result of the caging effect of the first coordination shell [24]. Caging effects are very visible instead in TB [7,8] which leads to too low a value of D. The lifetime of the first coordination shell is very short ($\sim$ 0.1 psec) and the long-time behavior is dominated by pairs of atoms that move together and exert small oscillations. There are small but detectable differences between the two sets of calculations. These are again consistent with the spin-induced strengthening of the covalent bond.

In conclusion, we have presented large-scale first-principles MD simulations of ℓ-Si close to the melting point. The main result of the study is that spin has an appreciable effect on the description of the attractive part of the interatomic potential. This leads to a modification of the description of weak bonds and hence of the structure, bonding, and properties of ℓ-Si. It is tempting to try to explain the anomalous density increase above the melting point as well as the anomalies in the other properties [5] in terms of existence of a "covalent network" induced by increased spin fluctuations close to the melting point. In situations such as that of ℓ-Si where experiments are difficult and subject to significant uncertainties it is important to perform calculations with accuracy that can rival the experimental one. In these cases inclusion of spin fluctuations is indispensable to reach the required precision.

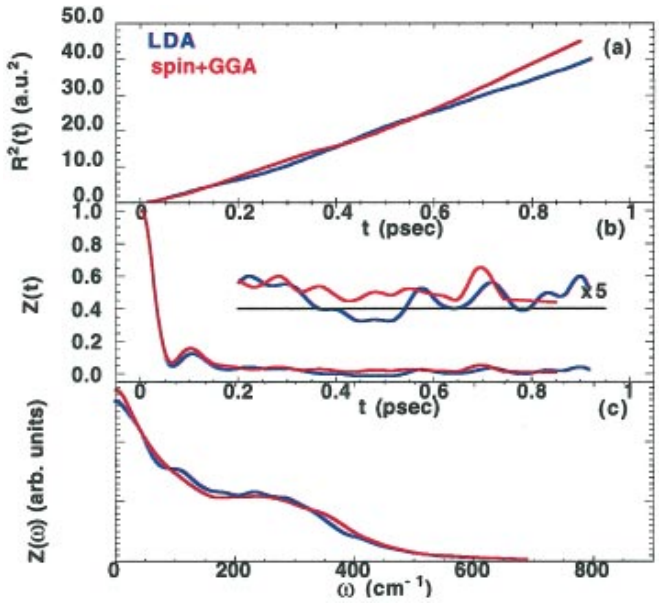

FIG. 6 (color). Dynamical properties: (a) mean-square displacement, (b) velocity autocorrelation function, and (c) the corresponding power spectrum. The inset in (b) shows the tails of $Z(t)$ on an expanded scale.

The calculations were performed on the JRCAT supercomputer system. I. S. thanks Dr. S. Kimura and his "Metamelt" project for suggesting this project and for his constant interest and encouragement. This work was partly supported by New Energy and Industrial Technology Development Organization (NEDO).

[1] Y. Waseda and K. Suzuki, Z. Phys. B **20**, 339 (1975).
[2] J. P. Gabathuler and S. Steeb, Z. Naturforsch **34A**, 1314 (1979).
[3] S. Takeda (to be published).
[4] V. M. Glazov, S. N. Chizhevskaya, and N. N. Glagoleva, *Liquid Semiconductors* (Plenum, New York, 1969).
[5] H. Sasaki *et al.*, Jpn. J. Appl. Phys. **33**, 3803 (1994); **34**, 3432 (1995); S.-I. Chung *et al.*, *ibid.* **34**, L631 (1995).
[6] J. Q. Broughton and X. P. Li, Phys. Rev. B **35**, 9120 (1987); W. D. Luedtke and U. Landman, *ibid.* **37**, 4656 (1988); **40**, 1164 (1989).
[7] R. Virkunen, K. Laasonen, and R. M. Nieminen, J. Phys. Condens. Matter **3**, 7455 (1991).
[8] C. Z. Wang, C. T. Chan, and K. M. Ho, Phys. Rev. B **45**, 12 227 (1992).
[9] G. Servalli and L. Colombo, Europhys. Lett. **22**, 107 (1993).
[10] I. Štich, M. Parrinello, and R. Car, Phys. Rev. Lett. **63**, 2240 (1989); Phys. Rev. B **44**, 4262 (1991).
[11] J. R. Chelikowsky and N. Binggeli, Solid State Commun. **88**, 381 (1993).
[12] G. Kresse and J. Hafner, Phys. Rev. B **49**, 14 251 (1994); N. Takeuchi and I. L. Garzón, *ibid.* **50**, 8342 (1994).
[13] O. Gunarson and B. I. Lundqvist, Phys. Rev. B **13**, 4274 (1976).
[14] J. P. Perdew and A. Zunger, Phys. Rev. B **23**, 5048 (1981).
[15] J. P. Perdew *et al.*, Phys. Rev. B **46**, 6671 (1992).
[16] A. Filipponi and A. Di Cicco, Phys. Rev. B **51**, 12 322 (1995).
[17] L. J. Clarke, I. Štich, and M. C. Payne, Comput. Phys. Commun. **72**, 14 (1992).
[18] M. C. Payne *et al.*, Rev. Mod. Phys. **64**, 1045 (1993).
[19] J. A. White and D. M. Bird, Phys. Rev. B **50**, 4954 (1994).
[20] S. Nosé, J. Chem. Phys. **81**, 511 (1984).
[21] J. Fortner and J. S. Lannin, Phys. Rev. B **39**, 5527 (1989).
[22] The experimental $g(r)$'s are, similarly to the coordination numbers, subject to large uncertainties.
[23] I. Štich, R. Car, and M. Parrinello, Phys. Rev. B **44**, 11 092 (1991).
[24] J. P. Boon and S. Yip, *Molecular Hydrodynamics* (McGraw-Hill, New York, 1980).